

# Sputtered gas-phase dianions detected by high-sensitivity mass spectrometry

Hubert Gnaser <sup>a,\*</sup>, Robin Golser <sup>b</sup>

<sup>a</sup> *Fachbereich Physik und Institut für Oberflächen- und Schichtanalytik, Technische Universität Kaiserslautern, D-67663 Kaiserslautern, Germany*

<sup>b</sup> *Vienna Environmental Research Accelerator, Institut für Isotopenforschung und Kernphysik, Universität Wien, A-1090 Wien, Austria*

Received 26 April 2006; accepted 24 May 2006

Available online 6 June 2006

## Abstract

The detection of small doubly-charged molecular anions by means of highly sensitive mass spectrometry is discussed. The production of these gas-phase dianions is accomplished by sputtering the specimen with  $\text{Cs}^+$  ions with an energy of a few keV. It is demonstrated that dianions can be detected most easily when the molecular ion has an odd total mass; then, the dianions will show up at half-integral mass numbers in the mass spectrum. In addition, the agreement of the relative abundances of several isotopomers of a dianion with the nominal isotopic pattern corroborates the identification of a dianionic species in the mass spectrum. These features are exemplified by monitoring mixed silicon–oxygen dianions of the general form  $\text{Si}_n\text{O}_{2n+1}^{2-}$  (with  $2 \leq n \leq 8$ ) in a low-energy mass spectrometer. They were formed by sputtering a silicon wafer at an elevated oxygen partial pressure in the vicinity of the sample's surface. The flight time through the mass spectrometer of  $\sim 15\text{--}30\ \mu\text{s}$  establishes a lower limit with respect to the intrinsic lifetimes of these dianions. Emission energy spectra of various singly- and doubly-charged ions illustrate the occurrence of fragmentation processes. The yields of the doubly- and singly-charged mixed silicon–oxygen anions increase with the ratio of the  $\text{O}_2$  arrival rate to the  $\text{Cs}^+$  flux density, but tend to saturate when this ratio approaches unity. The benefits of high-energy accelerator mass spectrometry in dianion detection are illustrated for  $\text{LiF}_3^{2-}$  and  $\text{CaF}_4^{2-}$ .

© 2006 Published by Elsevier B.V.

PACS: 36.40.-c; 79.20.Rf; 33.15.Ta; 82.80.Ms

Keywords: Dianions; Sputtering; Mass spectrometry; Energy spectra

## 1. Introduction

The existence of doubly-charged anions or, more generally, of multiply charged anions (MCAs) in the gas phase has attracted considerable theoretical and experimental attention [1–7]. Small dianions and trianions (such as  $\text{O}^{2-}$ ,  $\text{CO}_3^{2-}$ ,  $\text{SO}_4^{2-}$ , or  $\text{PO}_4^{3-}$ ) are ubiquitous in solutions and in the solid state and, naturally, are of paramount importance in physics, chemistry and biochemistry. However, as Cederbaum and Dreuw [6] noted: “Although these species exist in condensed phases, it is rather unlikely that

they represent stable gas-phase MCAs due to the strong electrostatic repulsion of the excess electrons. The Coulomb repulsion strongly favors the emission of one electron and supports the dissociation of the molecular framework into two monoanionic fragments.” Theoretical work [8–10] indeed corroborates this statement.

From a theoretical point of view, a stable gas-phase MCA must possess two basic properties: first, it must be stable with respect to electron autoejection and second, it must be stable with respect to fragmentation of the nuclear framework. Both of these decay channels are strongly supported by the electrostatic repulsion of the excess negative charges. Thus, the existence of small MCAs in the gas phase is very unlikely, while it is not surprising that the accommodation of two or more additional electrons

\* Corresponding author.

E-mail address: [gnaser@rhrk.uni-kl.de](mailto:gnaser@rhrk.uni-kl.de) (H. Gnaser).

becomes more probable when the molecular size increases. In fact, evidence for the existence of large organic molecular dianions was already reported more than three decades ago [11].

The first unambiguous observation by Schauer et al. [12], of *small, long-lived* dianionic species in the gas phase reported the generation of  $C_n^{2-}$  ( $n = 7\text{--}28$ ) by sputtering and their detection by mass spectrometry, implying lifetimes of at least some  $10^{-5}$  s. The existence of these dianions was later confirmed [13,14] and studied [15,16] in some detail by other groups. That observation triggered a search for other MCAs by theoretical and experimental means. Theoretical investigations were pioneered by Cederbaum and his coworkers. In a series of papers, this group [17–25] has shown that small doubly-charged negative clusters might indeed be stable in the gas phase, albeit with rather small binding energies. The smallest dianionic molecules identified to be stable in these calculations were  $MX_3^{2-}$  ( $M = \text{Li, Na, K; X = F, Cl}$ ) [18–20,26] and  $MX_4^{2-}$  ( $M = \text{Be, Mg, Ca; X = F, Cl}$ ) [17,22],  $C_n^{2-}$  [21,23],  $Si_nO_m^{2-}$  [27],  $Si_2O_5^{2-}$  [28],  $S_n^{2-}$  [29],  $SiC_6^{2-}$  [30],  $BeC_n^{2-}$  [31], and  $PtX_6^{2-}$  ( $X = \text{F, Cl, Br}$ ) [32]. More recent work of this group investigated the existence of long-lived dianions containing tetrahedrally coordinated oxygen atoms, namely,  $O(C_2)_4^{2-}$  and  $O(BN)_4^{2-}$  [33], of cyclic carbon cluster dianions [34], of tetraborates [35], of derivatives of the *closo*-hexaborate dianion  $B_6H_6^{2-}$  [36], and of aromatic dianions [37]. Apart from identifying (meta)stable dianions, these computations indicated a possible general formation principle: small dianions are expected to be particularly stable if they consist of a central, at least partially positively charged atom and several *equivalent* negatively charged ligands [2,6,30,38]. Furthermore, it was pointed out [31,39,40] that for multiply charged anions a repulsive Coulomb barrier for electron emission exists which may result in small *meta-stable* dianions which can be detected by mass spectrometry. In fact, the existence of such a Coulomb barrier was inferred from various experiments [41–47]. Apart from dianions, Cederbaum and coworkers studied different small MCAs [19,24,25,48–50].

Theoretical work by other groups [51–59] corroborated and diversified these results.

Following the experimental detection of  $C_n^{2-}$  [12], several different types of other dianions were produced by means of *sputtering*:  $SiC_n^{2-}$  ( $n = 6, 8, 10$ ) [60],  $BeC_n^{2-}$  ( $4 \leq n \leq 14$ ) [61,62],  $OC_n^{2-}$  ( $5 \leq n \leq 19$ ) [63,64],  $SC_n^{2-}$  ( $6 \leq n \leq 18$ ) [65],  $BeF_4^{2-}$  and  $MgF_4^{2-}$  [66],  $CaF_4^{2-}$  [67],  $HfF_6^{2-}$  [68],  $ZrF_6^{2-}$  [65],  $LiF_3^{2-}$  [69],  $Be_{n-1}O_n^{2-}$  ( $n = 4, 6$ ), and  $CuBe_2O_4^{2-}$  [70], as well as a few others [65,71]. However, also a considerable number of unsuccessful searches for dianions were reported [13,65,68,72].

Apart from sputtering, other ways of dianion formation were employed: Oxygen cluster ( $O_2$ ) $_n^{2-}$  ( $n = 3, 5, 7, 9$ ) were formed by electron attachment to an  $O_2$  beam [73]. *Electrospray ionization* was used to produce various dianions, e.g.,  $SO_4^{2-} \cdot nH_2O$ ,  $S_2O_6^{2-} \cdot nH_2O$ , and  $S_2O_8^{2-} \cdot nH_2O$  [74],  $MX_4^{2-}$  ( $M = \text{Pd, Pt; X = Cl, Br}$ ) [43,44,75],  $MX_6^{2-}$  ( $M = \text{Re, Os,$

$\text{Ir, Pt; X = Cl, Br}$ ) [43,76],  $ZrF_6^{2-}$  [77] or aliphatic dicarboxylate dianions [78–80]. While fullerene dianions (with  $n = 70\text{--}124$ ) [81] and even  $C_{60}^{3-}$  and  $C_{60}^{4-}$  [82] could be produced by electrospray mass spectrometry, no  $C_{60}^{2-}$  dianions were observed in these studies. Doubly-charged  $C_{60}^{2-}$  and  $C_{70}^{2-}$  ions have been produced also by *laser desorption* [83,84] or by collisions with Na atoms [85] whereas  $C_{60}F_{48}^{2-}$  [41],  $C_{84}^{2-}$  [42],  $C_{76}^{2-}$  [86], and  $C_{70}^{2-}$  [87] could be formed by electron attachment. More recently, dianions and even trianions of *large* metal clusters (some 30 or more constituents) could be produced by laser ablation [88] or by metal evaporation and subsequent *electron attachment* [89–92].

The aim of the present work is to discuss the production of dianions in the gas phase by sputtering and to describe their detection both in conventional mass spectrometers, operated at ion-beam energies of a few keV and in high-energy mass spectrometry. For the former, the pertinent aspects will be illustrated by means of a new class of molecular dianions,  $Si_nO_{2n+1}^{2-}$ , with  $2 \leq n \leq 8$  [93]. These ions species were produced by sputtering a silicon wafer with  $Cs^+$  primary ions in an oxygen ambient of about  $1 \times 10^{-5}$  mbar, in the same way as it was done before for the production of  $OC_n^{2-}$  dianions [63–65]. Some benefits for the identification of dianions at MeV-energies using accelerator mass spectrometry will be pointed out and discussed with respect to the detection of  $LiF_3^{2-}$  and  $CaF_4^{2-}$  dianions.

## 2. Experimental

The low-energy experiments were performed in a standard secondary-ion mass spectrometer (SIMS) instrument (Cameca IMS-4f [94]). Primary  $Cs^+$  ions are produced in a surface-ionization source and the ion beam is mass analyzed and focused by electrostatic lenses. For the present experiments, the beam current amounted to  $\sim 100\text{--}150$  nA and the beam size was  $\sim 50$   $\mu\text{m}$ . It was raster-scanned across a surface area of  $\sim 1.6 \times 10^{-4}$   $\text{cm}^2$ , resulting in  $Cs^+$  ion flux densities  $j(Cs^+) = (4\text{--}6) \times 10^{15}$  ions/ $\text{cm}^2$  s. The  $Cs^+$  impact energy was 14.5 keV. The sample is at a potential of  $-4500$  V and faces a grounded (extraction) electrode, which causes an acceleration of the emitted negative ions to an energy of  $(4.5 \times q)$  keV, with  $q$  being the ions' charge state. The field strength in this region is 10 kV/cm. Upon passing the extraction electrode, the beam of negative secondary ions is focused by electrostatic lenses onto the entrance slit of the mass spectrometer proper. It consists of an electrostatic (spherical condenser) and a magnetic sector field both with a  $90^\circ$  deflection of the beam. Ions of the correct energy-to-charge and mass-to-charge ratio pass the mass spectrometer exit slit and are detected, upon being subjected to another  $90^\circ$  deflection in an electrostatic sector, by a discrete-dynode electron multiplier. Even with all slits fully open this triple-deflection of the beam results in a negligible *mass-independent* background ( $< 1$  count in 10 s). The present results were obtained at a low mass resolution of  $M/\Delta M_{0.1} \sim 300\text{--}600$

( $\Delta M_{0.1}$  corresponds to the width of a mass peak at 10% of its maximum intensity), but a much higher resolution (up to  $M/\Delta M_{0.1} \sim 13,000$  [95]) can be achieved by closing both the entrance and exit slits of the spectrometer.

Energy spectra in the present work were recorded by ramping the target potential (up to  $\pm 125$  V around its nominal value of  $-4500$  V) and keeping the other optical elements of the secondary-ion beam line unchanged. With the energy slit closed, then only ions whose kinetic (emission) energy and the actual sample potential add up to  $4500$  eV can pass the slit and are being detected; the energy resolution then amounts to  $\sim 2\text{--}3$  eV.

The oxygen partial pressure  $p(\text{O}_2)$  in the vicinity of the specimen could be increased, from its base value well below  $\sim 1 \times 10^{-9}$  mbar, in a controlled fashion by introducing oxygen into the sample chamber via an ultra-high-vacuum leak valve. The maximum value used in this experiment was  $p(\text{O}_2) = 2.5 \times 10^{-5}$  mbar; at this partial pressure the arrival rate of  $\text{O}_2$  molecules amounts to  $j(\text{O}_2) \sim 6.7 \times 10^{15}$  molecules/cm<sup>2</sup>s. As discussed below, an important quantity in this context is the ratio of the  $\text{O}_2$  arrival rate and of the  $\text{Cs}^+$  flux density,  $R = j(\text{O}_2)/j(\text{Cs}^+)$ . The specimen used was a Si wafer; upon insertion into the instrument, the surface was cleaned by sputtering. The measurements reported in the following refer to steady-state sputtering.

The high-energy measurements have been performed at the Vienna Environmental Research Accelerator (VERA), an accelerator mass spectrometer with a terminal voltage of up to  $3$  MeV (manufactured by National Electrostatics Corporation). The ion source is optimized for high output and produces  $\text{Cs}^+$ -currents of the order of  $0.5$  mA in close vicinity of the samples. The major components of the low-energy side are a  $45^\circ$  spherical electrostatic analyzer and a  $90^\circ$  double-focusing injection magnet. Passing these devices, negative ions are then accelerated in a  $3$  MV Pelletron tandem accelerator and stripped to positive ions at the terminal stripper operated with Ar or  $\text{O}_2$ . At the high-energy side, VERA is equipped with a  $90^\circ$  double-focusing analyzing magnet and a  $90^\circ$  spherical electrostatic analyzer with  $2.0$  m bending radius. For the measurements of dianions, a silicon surface-barrier detector is used. A detailed description of this instrument is given in [96,97].

### 3. Results and discussion

By their very nature, dianions are usually formed with low probability. In order to monitor them by mass spectrometry, ion formation and detection has to be maximized. It is well established [98] that  $\text{Cs}^+$  bombardment of solids (and the concurrent incorporation of cesium into the near-surface region [99]) causes a prolific generation and emission of *negative* ions from that material. This finding is generally ascribed to a lowering of the sample's work function [100] that, in turn, increases (exponentially) the ionization probability of the sputtered species [98]. This yield enhancement has been shown [101] to be valid also

for cluster ions and is of particular importance for the sensitive detection of ions which intrinsically form with low probability such as dianions. Hence, a  $\text{Cs}^+$  ion beam is generally utilized for the detection of sputtered anions.

Following the original approach in [12], essentially all experiments carried out to detect doubly-charged negative ions in mass spectrometry, both at low and at high energies, used molecular species with an *odd* total mass  $M$ . Dianions are then observed at *half-integral* mass numbers in the spectrum as the electrical and magnetic elements employed always specify the mass-to-charge ratio ( $M/q$ ). In addition, this provides the possibility to work at low mass resolution and, hence, at a high instrument transmission. While the detection of a mass peak at a *half-integral* mass number is usually a very strong indication for the presence of a dianion in the mass spectrometer, some ambiguities may still arise and this will be discussed below.

Fig. 1 exemplifies this detection scheme for the most abundant mixed silicon–oxygen dianion,  $\text{Si}_3\text{O}_7^{2-}$ . Three distinct peaks at half-integral mass numbers are seen in the spectrum, at  $98.5$ ,  $99.5$ , and  $100.5$  amu; their relative intensities are  $1:9.0 \times 10^{-2}:1.7 \times 10^{-3}$ . Following the above argument, we can assume that these are caused by dianions with an odd total mass. Both silicon and oxygen have three stable isotopes:  $^{28}\text{Si}$ ,  $^{29}\text{Si}$ ,  $^{30}\text{Si}$  and  $^{16}\text{O}$ ,  $^{17}\text{O}$ ,  $^{18}\text{O}$ , respectively. Hence, various combinations of them can lead to an odd mass in a  $\text{Si}_3\text{O}_7^{2-}$  dianion. Because of their (largely) different isotopic abundances, a clear identification is possible. Using a polynomial distribution to compute the abundances, the three most abundant  $\text{Si}_3\text{O}_7^{2-}$  isotopomers with an odd total mass that can produce the peaks at these half-integral mass numbers are:  $^{28}\text{Si}_2^{29}\text{Si}^{16}\text{O}_7^{2-}$  at  $98.5$  amu,  $^{28}\text{Si}^{29}\text{Si}^{30}\text{Si}^{16}\text{O}_7^{2-}$  at  $99.5$  amu, and  $^{29}\text{Si}^{30}\text{Si}_2^{16}\text{O}_7^{2-}$

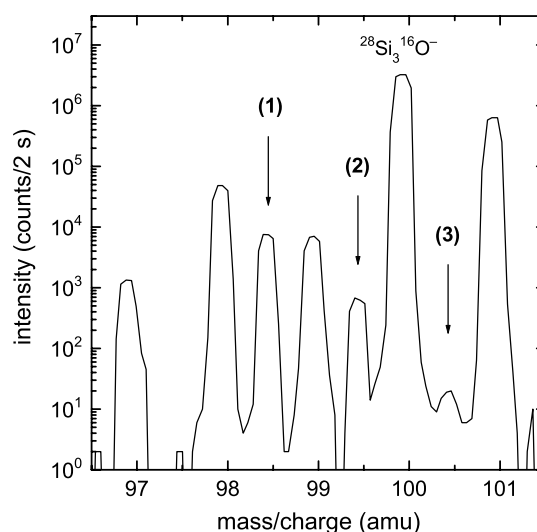


Fig. 1. Mass spectrum in the range of the most abundant mixed silicon–oxygen dianion,  $\text{Si}_3\text{O}_7^{2-}$ ; the arrows indicate the isotopomers observed at half-integral mass numbers: (1)  $^{28}\text{Si}_2^{29}\text{Si}^{16}\text{O}_7^{2-}$  at  $98.5$  amu, (2)  $^{28}\text{Si}^{29}\text{Si}^{30}\text{Si}^{16}\text{O}_7^{2-}$  at  $99.5$  amu, and (3)  $^{29}\text{Si}^{30}\text{Si}_2^{16}\text{O}_7^{2-}$  at  $100.5$  amu. The data were obtained by  $14.5$ -keV  $\text{Cs}^+$  ion bombardment of a silicon wafer at an elevated oxygen partial pressure of  $p(\text{O}_2) \sim 10^{-5}$  mbar.

at 100.5 amu. At 99.5 and 100.5 amu, two other isotopomers contribute to the signals:  $^{28}\text{Si}_2^{29}\text{Si}^{16}\text{O}_6^{2-}$  and  $^{28}\text{Si}^{29}\text{Si}^{30}\text{Si}^{16}\text{O}_6^{2-}$ , but their abundances are lower by factors of 39 and 9.8, respectively. The computed relative isotopic pattern of these three mass peaks is then:  $1:8.3 \times 10^{-2}:2.2 \times 10^{-3}$ . These ratios are rather close to the above given measured relative intensities of these peaks. This agreement provides essentially undisputable evidence that  $\text{Si}_3\text{O}_7^{2-}$  dianions produced by sputtering are detected in the spectrum shown in Fig. 1.

Principally, the mass peaks at the integral mass numbers 98 and 99 amu in Fig. 1 can result from any singly-charged molecular species, such as the peak at 100 amu which is due to the  $^{28}\text{Si}_3^{16}\text{O}^-$  anion. However, the measured intensity ratio of the peaks at 98 and 98.5 amu ( $\sim 6.4$ ) agrees very well with the computed abundance pattern of the  $^{28}\text{Si}_3^{16}\text{O}_7^{2-}$  and  $^{28}\text{Si}_2^{29}\text{Si}^{16}\text{O}_7^{2-}$  isotopomers (6.44). Therefore, the signal at 98 amu can be assumed to be largely due to  $^{28}\text{Si}_3^{16}\text{O}_7^{2-}$ . For the peak at 99 amu, the measured ratio relative to 98.5 is 0.94, whereas the nominal dianion ratio of  $^{28}\text{Si}_2^{29}\text{Si}^{16}\text{O}_7^{2-}$  (at 99 amu) to  $^{28}\text{Si}_2^{29}\text{Si}^{16}\text{O}_7^{2-}$  (at 98.5 amu) amounts to 0.80. This difference indicates that, apart from the dianion, another ion species contributes to the signal detected at 99 amu.

Fig. 2 shows a mass spectrum in the range of the smallest  $\text{Si}_n\text{O}_{2n+1}^{2-}$  dianion detected,  $\text{Si}_2\text{O}_5^{2-}$ ; it is monitored as  $^{28}\text{Si}^{29}\text{Si}^{16}\text{O}_5^{2-}$  at 68.5 amu. However, the intensity is too low for this species to detect other isotopomers of this kind, e.g.,  $^{29}\text{Si}^{30}\text{Si}^{16}\text{O}_5^{2-}$  at 69.5 amu. The experimental observation of this dianion corroborates the theoretical prediction of its stability by Cederbaum and coworkers some 10 years ago [28].

Using these data and similar ones for other cluster ions, their abundance distribution can be established. Fig. 3 depicts the yields of  $\text{Si}_n\text{O}_{2n+1}^{2-}$  dianions as a function of

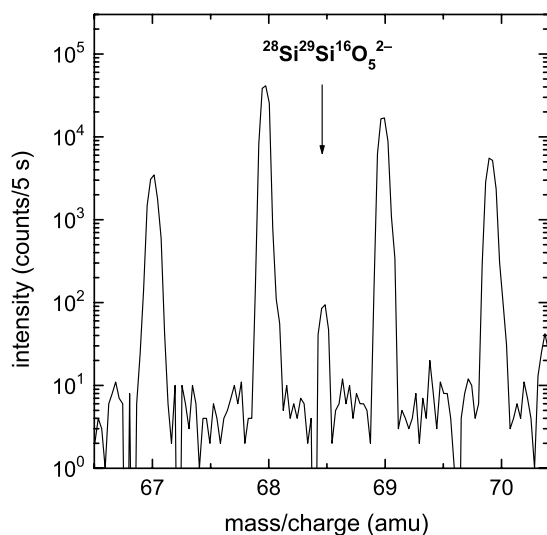


Fig. 2. Mass spectrum in the range of the  $\text{Si}_2\text{O}_5^{2-}$  dianion, obtained by 14.5-keV  $\text{Cs}^+$  ion bombardment of a silicon wafer at an elevated oxygen partial pressure of  $p(\text{O}_2) \sim 10^{-5}$  mbar.

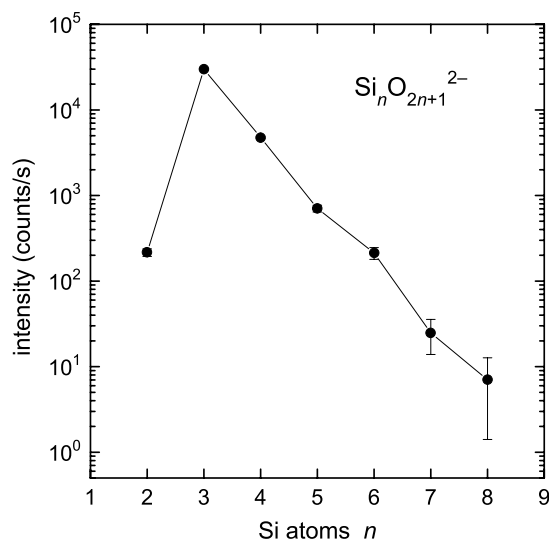


Fig. 3. Intensities of  $\text{Si}_n\text{O}_{2n+1}^{2-}$  dianions as a function of the number of silicon atoms,  $n$ . The intensities are corrected for the isotopic abundances of the isotopomers monitored. The data were taken at a value  $R \sim 1$ .

the number of Si-atoms,  $n$ , in the cluster, with  $2 \leq n \leq 8$ . No doubly-charged ions of this form with smaller or larger  $n$  could be found. However, another mixed silicon–oxygen dianion,  $\text{Si}_5\text{O}_{10}^{2-}$ , was observed as  $^{28}\text{Si}_4^{29}\text{Si}^{16}\text{O}_{10}^{2-}$  at 150.5 amu.

Apart from the dianions described so far also singly charged negative molecular ions were observed, containing various numbers of Si and O atoms. In the present experiment, the intensities of sputtered O-carrying molecules (charged or neutral) depend on the arrival rate of  $\text{O}_2$ -molecules at the surface. This is due to the fact that, for a fixed  $\text{Cs}^+$  flux density, the value of  $j(\text{O}_2)$  determines the stationary oxygen surface coverage. (The sticking coefficient of  $\text{O}_2$  also influences the magnitude of the coverage.) The decisive quantity is therefore the ratio of the  $\text{O}_2$  arrival rate and of the  $\text{Cs}^+$  flux density,  $R = j(\text{O}_2)/j(\text{Cs}^+)$ . As the majority of sputtered species originate from the first and second monolayer of the surface, the intensities of O-carrying molecules may saturate at an oxygen coverage approaching unity. The dependence of the yields of some selected  $\text{Si}_n\text{O}_m^-$  and  $\text{Si}_n\text{O}_{n+1}^{2-}$  ions as a function of  $R$  are depicted in Fig. 4. The data indicate that in general the ion yields increase with  $R$  and tend to saturate for  $R \sim 1$ . Therefore, all data shown in Figs. 1–3 were recorded at  $R \sim 1$ .

The saturation in oxygen coverage can be inferred also from the fact that the  $\text{Si}^-$  starts to decrease above  $R \sim 0.5$ . It should be noted in this context that covering the surface (partially) by oxygen may influence also the ionization probability of sputtered species. The effect is very pronounced for positive ion emission [98], but is found occasionally also for anions, albeit to a much smaller degree.

In several previous investigations on the emission of sputtered clusters and molecules [99] it was noted that fragmentation in the sputtering event may have an influence on

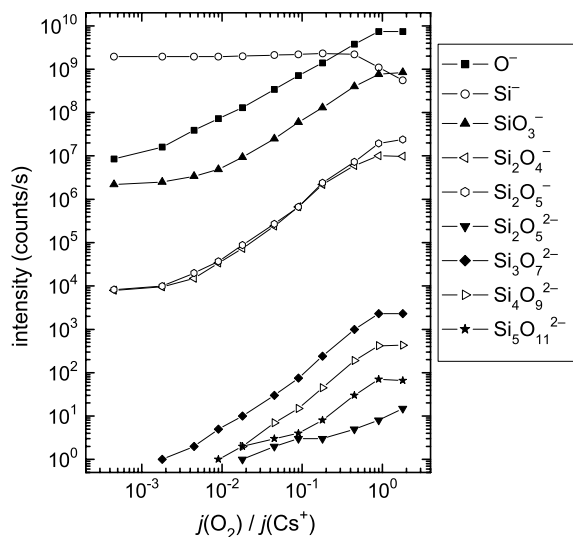


Fig. 4. The yields of  $\text{O}^-$  and  $\text{Si}^-$ , and of several singly- and doubly-charged negative molecular ions as a function of the ratio of the  $\text{O}_2$  arrival rate to the  $\text{Cs}^+$  flux density,  $R = j(\text{O}_2)/j(\text{Cs}^+)$ .

the cluster size distributions. It is well documented [102] that clusters are generally sputter ejected “hot”, i.e., with a high degree of internal excitation; following ejection, they are cooling by evaporation of small entities (atoms or dimers). This process of fragmentation was investigated in detail for  $\text{C}_n^-$  and  $\text{C}_n^{2-}$  cluster ions [16]. If such decomposition takes place in the accelerating region of the mass spectrometer, it can be readily monitored via the energy distributions of sputtered ions.

This approach was employed also in the present work, recording energy spectra for several singly- and doubly-charged mixed silicon–oxygen anions. Fig. 5 depicts the corresponding data. Generally, ion species with positive emission energies refer to stable ions and the measured energies correspond to their kinetic energy with which they are ejected from the surface. By contrast, “negative” emission energies are due to molecular ions that have not experienced the full acceleration potential, but are the product of an unimolecular fragmentation process [16,99]; the kinetic energy of the fragment ion is lowered and it will exit from the acceleration region with an energy deficit  $\Delta E$  with respect to a non-fragmenting species;  $\Delta E$  is related to the electrostatic potential  $V(z)$  at the point of fragmentation, a distance  $z$  downstream from the surface and its mass relative to that of the parent species [103,104].

Fig. 5a shows that such negative excursions are very pronounced in the spectra of all monoanions recorded, in agreement with many previous data for singly-charged anions [16,103,104]. While it is not possible to determine from data like those shown in Fig. 5 what kind of fragmentation reaction did occur, i.e., which parent and daughter ions were involved, these processes appear to be ubiquitous and they contribute pronouncedly to the detected ion flux, especially for larger molecules. Interestingly, a rather high signal is observed for the  $\text{Si}_3\text{O}_7^-$  anion at high positive emission energies. A similar observation for  $\text{C}_n^-$  [16] was ascribed to the

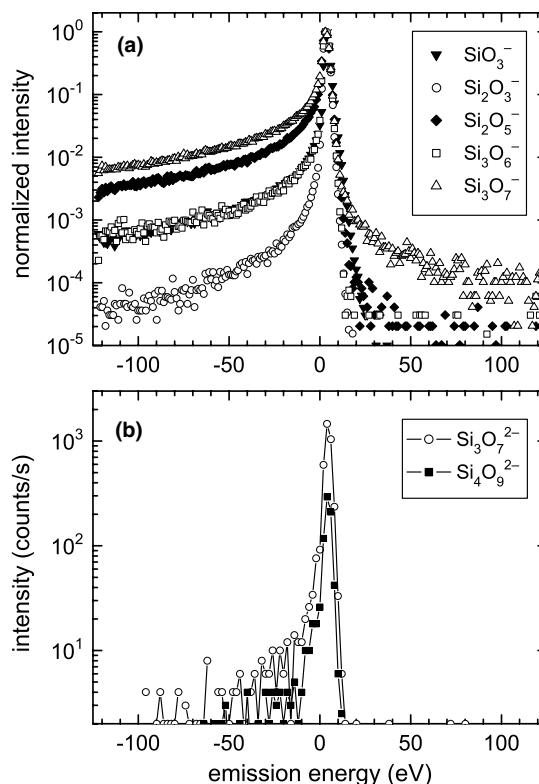


Fig. 5. Emission-energy spectra of several singly-charged silicon–oxygen molecular anions (a) and of the dianions  $\text{Si}_3\text{O}_7^{2-}$  and  $\text{Si}_4\text{O}_9^{2-}$  (b), sputtered from silicon by 14.5-keV  $\text{Cs}^+$  ion bombardment at an oxygen partial pressure of  $p(\text{O}_2) \sim 10^{-5}$  mbar. The signals at “negative” energies are due to fragment ions (see text for details).

fragmentation of dianion species: as a doubly-charged parent ion gains twice the energy in the accelerating field before fragmenting compared to a singly-charged ion, the decomposition process may result in singly-charged daughter ions with an energy surplus which will show up in the corresponding energy spectra at positive emission energies.

The energy spectra of the two dianions  $\text{Si}_3\text{O}_7^{2-}$  and  $\text{Si}_4\text{O}_9^{2-}$  shown Fig. 5b also indicate the presence of tails towards “negative” energies, albeit to a lesser extent. This observation contrasts with the respective data for  $\text{C}_n^{2-}$  dianions for which such negative excursions were absent [16]. In the present case, fragmentation processes which produce a doubly-charged daughter ion from a parent dianion, in analogy to the situation of singly-charged species, could explain this finding, but such a decay mechanism appears highly unlikely. The formation of dianions by electron attachment processes or electron transfer in gas-phase collisions near the emission site at the surface could produce such energy deficits.

While ions decomposing in the accelerating region cannot pass through the spectrometer under normal operation (i.e., with the sample potential  $V = -4500$  V), a possible problem in terms of the unambiguous detection of dianions could be envisaged: Let us, for example, consider a singly-charged  $\text{Si}_4\text{O}_{10}^-$  anion which, during its passage from the electrostatic to the magnetic sector, breaks up into two

fragments of equal mass ( $\text{Si}_2\text{O}_5^-$  and  $\text{Si}_2\text{O}_5$ ); then, the charged daughter ion possesses the same magnetic rigidity ( $ME/q^2$ ) as the doubly-charged  $\text{Si}_2\text{O}_5^{2-}$  and these two ion species could not be separated by the magnet; and the same would hold for any symmetrically decaying molecules. However, in the present instrument the final energy deflector in front of the detector might separate those species via their different energies. In addition, fragmentation processes will produce also other daughter ions (with unequal masses) which hence should show up in the mass spectrum at fractional mass numbers; the apparent absence of such mass peaks would then be a distinct indication that the signals detected are not due to a decomposition process. At this point, the necessity to use *half-integral* mass numbers for the detection of dianions by conventional (low-energy) mass spectrometry becomes obvious. Unfortunately, for several dianion species of interest the requirement that the total mass number of the molecule has to be odd cannot be fulfilled, e.g.,  $\text{KF}_3^{2-}$  or  $\text{KCl}_3^{2-}$ .

As compared to low-energy mass spectrometry, accelerator mass spectrometry (AMS) provides additional means to identify doubly-charged negative molecules. AMS allows to “analyze” a molecular dianion due to the break-up of the molecule into its atomic constituents during the stripping process in a tandem accelerator. The full strength shows up in cases for which the dianion under consideration is not part of series of similar dianionic species (such as  $\text{C}_n^{2-}$ ,  $\text{OC}_n^{2-}$ , or  $\text{Si}_n\text{O}_{2n+1}^{2-}$ ). Typical examples for that situation are  $\text{LiF}_3^{2-}$  and  $\text{CaF}_4^{2-}$ . Both could not be detected by low-energy mass spectrometry [13,68], but were later observed by AMS [67,69]. The experimental scheme will be discussed by means of one of the most coveted dianions produced by sputtering,  $\text{LiF}_3^{2-}$ , which is detected as  ${}^6\text{Li}^{19}\text{F}_3^{2-}$  at  $M/q = 31.5$  amu. When negative ions with  $M/q = 31.5$  amu are injected at the low-energy side of a tandem accelerator (running at 2.7 MV) and the high-energy side is set to detect  ${}^{19}\text{F}^{2+}$ , up to threefold coincidences are observed in an energy detector, cf. Fig. 6. Assuming the negative ions are in fact dianions of mass 63 amu, e.g.,  ${}^6\text{Li}^{19}\text{F}_3^{2-}$ , such a spectrum can be interpreted as follows: when a particular  ${}^6\text{Li}^{19}\text{F}_3^{2-}$  breaks up in the stripper, each of the atomic constituents  ${}^6\text{Li}$  and  ${}^{19}\text{F}$  starts a history of its own. So, after some interactions with the stripper gas, a  ${}^{19}\text{F}$  will exit in charge state 2+ with a certain probability. Since the high-energy side is set to  ${}^{19}\text{F}^{2+}$ , it will eventually be registered in the energy detector. The total energy measured in the detector depends on the fate of the other  ${}^{19}\text{F}$  from this very dianion. If only one out of the three  ${}^{19}\text{F}$  leaves the stripper in charge state 2+ and comes into the detector, the multi-channel-analyzer counts it in the peak corresponding to the particle energy, say  $E_1$  (around channel 200 in Fig. 6, labeled 1F). If two out of the three  ${}^{19}\text{F}$  go into 2+, they may hit the detector simultaneously, yielding  $2E_1$  and thus contributing a peak at twice the energy (around channel 400 in Fig. 6, labeled 2F). With a certain probability, even all three  ${}^{19}\text{F}$  from one particular  ${}^6\text{Li}^{19}\text{F}_3^{2-}$  may coincide. It is important to note that the

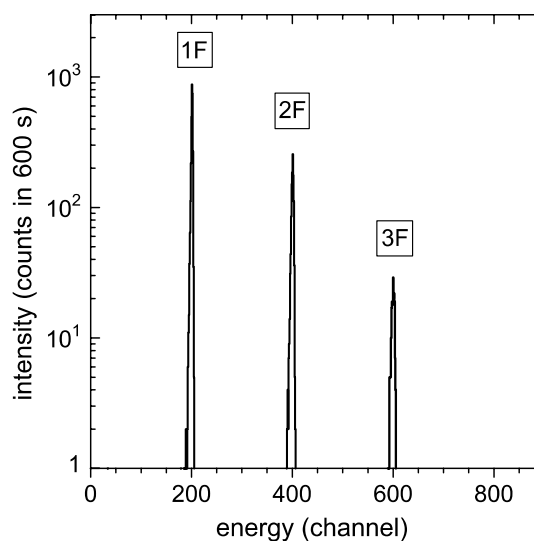


Fig. 6. Energy spectrum measured in a surface barrier detector when negative ions with  $M/q = 31.5$  amu, e.g.,  ${}^6\text{Li}^{19}\text{F}_3^{2-}$ , sputtered from enriched  ${}^6\text{LiF}$  are injected into the low-energy side of the accelerator and the high-energy side is set to detect  ${}^{19}\text{F}^{2+}$ .

peak-to-peak ratios would not change with source output. This is to be distinguished from pile-up, i.e., the random coincidence of  ${}^{19}\text{F}^{2+}$  from different molecules. Indeed, coincidences up to three-fold are observed when ions with  $M/q = 31.5$  are injected into the accelerator during sputtering of  $\text{LiF}$  (enriched in  ${}^6\text{Li}$  to more than 90%), see Fig. 6. This observation proves that the signal at  $M/q = 31.5$  contains molecular ions with three  ${}^{19}\text{F}$  atoms, that must be dianions as their masses add up to 57 amu. The remaining mass must then be 6 amu which can only be  ${}^6\text{Li}$ .

Another example,  $\text{CaF}_4^{2-}$  was examined using  ${}^{43}\text{Ca}^{19}\text{F}_4^{2-}$  (the only isotopomer with odd total mass) with  $M/q = 119/2 = 59.5$  amu. Injecting ions with this mass-to-charge into the accelerator and setting the high-energy side to monitor  ${}^{19}\text{F}^+$ , up to fourfold coincidences were observed in the detector [67], in agreement with expectations. However, when four  ${}^{19}\text{F}$  simultaneously arrive from a molecule with apparent mass 59.5 amu (smaller than 76 amu, i.e.,  $\text{F}_4$ ), the molecule can only be a dianion with mass 119 amu, and the remaining constituents must together have mass 43 amu. Whether the remainder is  ${}^{43}\text{Ca}$  (or something else, e.g.,  ${}^{27}\text{Al}^{16}\text{O}$ ) can be inferred from the additional information provided by mass scans at the low-energy side and at the high-energy side. For example, a clear peak in the count rate of  $43^+$  must show up at the high-energy side, when negative ions with apparent mass 59.5 amu are injected. This was indeed the case. Both signatures together, the correct multiplicity of coincidences in the energy detector and the observation of the residual species of the original molecule ( ${}^{43}\text{Ca}$  in the case of  ${}^{43}\text{Ca}^{19}\text{F}_4^{2-}$  and  ${}^6\text{Li}$  for  ${}^6\text{Li}^{19}\text{F}_3^{2-}$ ), provided the means for an unambiguous verification of the existence of those extremely elusive dianions.

This approach of AMS was first employed for the detection of dianions by Middleton and Klein [15], and was applied later by other groups [67,69,105,106].

#### 4. Conclusions

The general principles for the detection of small gas-phase dianions by low-energy mass spectrometry are outlined. Many molecular dianions could be produced with sufficient abundance by sputtering using  $\text{Cs}^+$  ions. Their unambiguous identification is typically possible if an isotopomer with an odd total mass can be monitored; the dianion appears then at a half-integral mass number in the spectrum. In favorable cases, several isotopomers can be detected and compared with their nominal isotopic abundance pattern for an additional verification. The dianions' flight time through the mass spectrometer of some 10  $\mu\text{s}$  constitutes a lower limit in terms of the intrinsic life times. Fragmentation processes of singly- and doubly-charged anions can be studied in some detail by recording emission-energy distributions. In such spectra, "negative" energies indicate the occurrence of decomposition reactions close to the emission site. In the present work, these experimental aspects are illustrated for the detection of the mixed silicon–oxygen molecular dianions,  $\text{Si}_n\text{O}_{2n+1}^{2-}$ , with  $2 \leq n \leq 8$ . These were produced by  $\text{Cs}^+$ -ion sputtering of a silicon wafer at an elevated oxygen pressure. Applying the same procedure using a Ge specimen, no dianions could be observed. Some advantages in the detection of dianions at MeV-energies using accelerator mass spectrometry are highlighted for two dianions of very low abundance,  $\text{LiF}_3^{2-}$  and  $\text{CaF}_4^{2-}$ .

#### Acknowledgement

The authors are grateful to Lorenz Cederbaum for many stimulating discussions and suggestions.

#### References

- [1] J. Kalcher, A.F. Sax, *Chem. Rev.* 94 (1994) 2291.
- [2] M.K. Scheller, R.N. Compton, L.S. Cederbaum, *Science* 270 (1995) 1160.
- [3] A.I. Boldyrev, M. Gutowski, J. Simons, *Acc. Chem. Res.* 29 (1996) 497.
- [4] G.R. Freeman, N.H. March, *J. Phys. Chem.* 100 (1996) 4331.
- [5] L.-S. Wang, X.-B. Wang, *J. Phys. Chem. A* 104 (2000) 1978.
- [6] A. Dreuw, L.S. Cederbaum, *Chem. Rev.* 102 (2002) 181.
- [7] D. Mathur, *Phys. Rep.* 391 (2003) 1.
- [8] R. Janoschek, *Z. Anorg. Allg. Chem.* 616 (1992) 101.
- [9] A.I. Boldyrev, J. Simons, *J. Phys. Chem.* 98 (1994) 2298.
- [10] T. Sommerfeld, *J. Phys. Chem. A* 104 (2000) 8806.
- [11] R.C. Dougherty, *J. Chem. Phys.* 50 (1969) 1896.
- [12] S.N. Schauer, P. Williams, R.N. Compton, *Phys. Rev. Lett.* 65 (1990) 625.
- [13] H. Gnaser, H. Oechsner, *Nucl. Instrum. Method B* 82 (1993) 518.
- [14] D. Calabrese, A.M. Covington, J.S. Thompson, *J. Chem. Phys.* 105 (1996) 2936.
- [15] R. Middleton, J. Klein, *Nucl. Instrum. Method B* 123 (1997) 532.
- [16] H. Gnaser, *Nucl. Instrum. Method B* 149 (1999) 38.
- [17] H.-G. Weikert, L.S. Cederbaum, F. Tarantelli, A.I. Boldyrev, *Z. Phys. D* 18 (1991) 299.
- [18] M.K. Scheller, L.S. Cederbaum, *J. Phys. B: At. Mol. Opt. Phys.* 25 (1992) 2257.
- [19] M.K. Scheller, L.S. Cederbaum, *Chem. Phys. Lett.* 216 (1993) 141.
- [20] M.K. Scheller, L.S. Cederbaum, *J. Chem. Phys.* 99 (1993) 441.
- [21] T. Sommerfeld, M.K. Scheller, L.S. Cederbaum, *Chem. Phys. Lett.* 209 (1993) 216.
- [22] H.-G. Weikert, L.S. Cederbaum, *J. Chem. Phys.* 99 (1993) 8877.
- [23] T. Sommerfeld, M.K. Scheller, L.S. Cederbaum, *J. Phys. Chem.* 98 (1994) 8914.
- [24] M.K. Scheller, L.S. Cederbaum, *J. Chem. Phys.* 101 (1994) 3962.
- [25] M.K. Scheller, L.S. Cederbaum, *J. Chem. Phys.* 100 (1994) 8934; M.K. Scheller, L.S. Cederbaum, *J. Chem. Phys.* 100 (1994) 8943.
- [26] T. Sommerfeld, M.S. Child, *J. Chem. Phys.* 110 (1999) 5670.
- [27] T. Sommerfeld, M.K. Scheller, L.S. Cederbaum, *J. Chem. Phys.* 103 (1995) 1057.
- [28] T. Sommerfeld, M.K. Scheller, L.S. Cederbaum, *J. Chem. Phys.* 104 (1996) 1464.
- [29] V. Berghof, T. Sommerfeld, L.S. Cederbaum, *J. Phys. Chem. A* 102 (1998) 5100.
- [30] A. Dreuw, T. Sommerfeld, L.S. Cederbaum, *J. Chem. Phys.* 109 (1998) 2727.
- [31] A. Dreuw, L.S. Cederbaum, *J. Chem. Phys.* 112 (2000) 7400.
- [32] T. Sommerfeld, S. Feuerbach, M. Pernpointner, L.S. Cederbaum, *J. Chem. Phys.* 118 (2003) 1747.
- [33] A. Dreuw, H. Schweinsberg, L.S. Cederbaum, *J. Phys. Chem. A* 106 (2002) 1406.
- [34] S. Feuerbach, A. Dreuw, L.S. Cederbaum, *J. Am. Chem. Soc.* 124 (2002) 3163.
- [35] A. Dreuw, N. Zint, L.S. Cederbaum, *J. Am. Chem. Soc.* 124 (2002) 10903.
- [36] N. Zint, A. Dreuw, L.S. Cederbaum, *J. Am. Chem. Soc.* 124 (2002) 4910.
- [37] T. Sommerfeld, *J. Am. Chem. Soc.* 124 (2002) 1119.
- [38] A. Dreuw, T. Sommerfeld, L.S. Cederbaum, *Angew. Chem. Int. Ed. Eng.* 36 (1997) 1889.
- [39] A. Dreuw, L.S. Cederbaum, *Phys. Rev. A* 63 (2001) 012501, and 049904(E).
- [40] J. Simons, P. Skurski, R. Barrios, *J. Am. Chem. Soc.* 122 (2000) 11893.
- [41] C. Jin, R.L. Hettich, R.N. Compton, A. Tuinman, A. Derecskei-Kovacs, D.S. Marynick, B.I. Dunlap, *Phys. Rev. Lett.* 73 (1994) 2821.
- [42] R.N. Compton, A.A. Tuinman, C.E. Klots, M.R. Pederson, D.C. Patton, *Phys. Rev. Lett.* 78 (1997) 4367.
- [43] X.-B. Wang, L.-S. Wang, *J. Chem. Phys.* 111 (1999) 4497.
- [44] X.-B. Wang, L.-S. Wang, *Phys. Rev. Lett.* 83 (1999) 3402.
- [45] X.-B. Wang, C.-F. Ding, L.-S. Wang, *Phys. Rev. Lett.* 81 (1998) 3351.
- [46] L.-S. Wang, C.-F. Ding, X.-B. Wang, *Rev. Sci. Instrum.* 70 (1999) 1957.
- [47] O.T. Ehrler, J. M. Weber, F. Furche, M.M. Kappes, *Phys. Rev. Lett.* 91 (2003) 113006.
- [48] A. Dreuw, L.S. Cederbaum, *J. Phys. Chem.* 105 (2001) 10577.
- [49] S. Feuerbach, L.S. Cederbaum, *J. Phys. Chem. A* 109 (2005) 11401.
- [50] S. Feuerbach, L.S. Cederbaum, *J. Chem. Phys.* 124 (2006) 044320.
- [51] E. Miyoshi, Y. Sakai, *J. Chem. Phys.* 89 (1988) 7363.
- [52] J.D. Watts, R.J. Bartlett, *J. Chem. Phys.* 97 (1992) 3445.
- [53] A.I. Boldyrev, J. Simons, *J. Chem. Phys.* 97 (1992) 2826.
- [54] A.I. Boldyrev, J. Simons, *J. Chem. Phys.* 98 (1993) 4745.
- [55] M. Gutowski, A.I. Boldyrev, J.V. Ortiz, J. Simons, *J. Am. Chem. Soc.* 116 (1994) 9262.
- [56] M. Gutowski, A.I. Boldyrev, J. Simons, J. Rak, J. Błazejowski, *J. Am. Chem. Soc.* 118 (1996) 1173.
- [57] Q. Shi, S. Kais, *J. Am. Chem. Soc.* 124 (2002) 11723.
- [58] C. Trindle, A. Yumak, *J. Chem. Theor. Comput.* 1 (2005) 433.
- [59] A. Dreuw, *Chem. Phys. Lett.* 419 (2006) 385.
- [60] H. Gnaser, *Phys. Rev. A* 60 (1999) R2645.
- [61] J. Klein, R. Middleton, *Nucl. Instrum. Method B* 159 (1999) 8.
- [62] D. Berkovits, O. Heber, J. Klein, D. Mitnik, M. Paul, *Nucl. Instrum. Method B* 172 (2000) 350.
- [63] H. Gnaser, *Phys. Rev. A* 66 (2002) 013203.

- [64] H. Gnaser, A. Dreuw, L.S. Cederbaum, *J. Chem. Phys.* 117 (2002) 7002.
- [65] K. Franzreb, P. Williams, *J. Chem. Phys.* 123 (2005) 224312.
- [66] R. Middleton, J. Klein, *Phys. Rev. A* 60 (1999) 3515.
- [67] R. Golser, H. Gnaser, W. Kutschera, A. Priller, P. Steier, C. Vockenhuber, A. Wallner, *Nucl. Instrum. Method B* 240 (2005) 468.
- [68] H. Gnaser, *Nucl. Instrum. Method B* 197 (2002) 49.
- [69] X.-L. Zhao, A.E. Litherland, *Phys. Rev. A* 71 (2005) 064501.
- [70] K. Franzreb, P. Williams, *Chem. Phys. Lett.* 419 (2006) 379.
- [71] R. Vandenbosch, D.I. Will, C. Cooper, B. Henry, J.F. Liang, *Chem. Phys. Lett.* 274 (1997) 112.
- [72] H. Gnaser, *Nucl. Instrum. Method B* 212 (2003) 407.
- [73] K. Leiter, W. Ritter, A. Stamatovic, T.D. Märk, *Int. J. Mass Spectrom. Ion Proc.* 68 (1986) 341.
- [74] A.T. Blades, P. Kebarle, *J. Am. Chem. Soc.* 116 (1994) 10761.
- [75] P. Weis, O. Hampe, S. Gilb, M.M. Kappes, *Chem. Phys. Lett.* 321 (2000) 426.
- [76] W.E. Boxford, M.O.A. El Ghazaly, C.E.H. Dessent, S.B. Nielsen, *Int. J. Mass Spectrom.* 244 (2005) 60.
- [77] X.-B. Wang, L.-S. Wang, *J. Phys. Chem. A* 104 (2000) 4429.
- [78] L.-S. Wang, C.-F. Ding, X.-B. Wang, J.B. Nicholas, *Phys. Rev. Lett.* 81 (1998) 2667.
- [79] C.-F. Ding, X.-B. Wang, L.-S. Wang, *J. Phys. Chem. A* 102 (1998) 8633.
- [80] X.-B. Wang, C.-F. Ding, L.-S. Wang, *Chem. Phys. Lett.* 307 (1999) 391.
- [81] O. Hampe, M. Neumaier, M.N. Blom, M.M. Kappes, *Chem. Phys. Lett.* 354 (2002) 303.
- [82] V. Cammarata, T. Guo, A. Illies, L. Li, P. Shevlin, *J. Phys. Chem. A* 109 (2005) 2765.
- [83] R.L. Hettich, R.N. Compton, R.H. Ritchie, *Phys. Rev. Lett.* 67 (1991) 1242.
- [84] P.A. Limbach, L. Schweikhard, K.A. Cowen, M.T. McDermott, A.G. Marshall, J.V. Coe, *J. Am. Chem. Soc.* 113 (1991) 6795.
- [85] B. Liu, P. Hvelplund, S.B. Nielsen, S. Tomita, *Phys. Rev. Lett.* 92 (2004) 168301.
- [86] J. Hartig, M.N. Blom, O. Hampe, M.M. Kappes, *Int. J. Mass Spectrom.* 229 (2003) 93.
- [87] A. Herlet, R. Jertz, J.A. Otamendi, A.J.G. Martínez, L. Schweikhard, *Int. J. Mass Spectrom.* 218 (2002) 217.
- [88] C. Stoermer, J. Friedrich, M.M. Kappes, *Int. J. Mass Spectrom.* 206 (2001) 63.
- [89] A. Herlert, S. Krückeberg, L. Schweikhard, M. Vogel, C. Walther, *Phys. Scripta T80* (1999) 200.
- [90] L. Schweikhard, A. Herlert, S. Krückeberg, M. Vogel, C. Walther, *Phil. Mag. B* 79 (1999) 1343.
- [91] C. Yannouleas, U. Landman, A. Herlert, L. Schweikhard, *Phys. Rev. Lett.* 86 (2001) 2996.
- [92] A. Herlert, L. Schweikhard, *Int. J. Mass Spectrom.* 229 (2003) 19.
- [93] In a note added in proof in Ref. [65], the authors report the detection of these species employing a procedure essentially identical to the present one.
- [94] H.N. Migeon, C. Le Pipec, J.J. Le Goux, in: A. Benninghoven, R.J. Colton, D.S. Simons, H.W. Werner (Eds.), *Secondary Ion Mass Spectrometry SIMSV*, Springer, Berlin, 1986, p. 155.
- [95] H. Gnaser, *Phys. Rev. A* 56 (1997) R2518.
- [96] C. Vockenhuber, I. Ahmad, R. Golser, W. Kutschera, V. Liechtenstein, A. Priller, P. Steier, S. Winkler, *Int. J. Mass Spectrom.* 223 (2003) 713.
- [97] P. Steier, R. Golser, W. Kutschera, A. Priller, C. Vockenhuber, S. Winkler, *Nucl. Instrum. Method B* 223–224 (2004) 67.
- [98] M.L. Yu, in: R. Behrisch, K. Wittmaack (Eds.), *Sputtering by Particle Bombardment III*, Springer, Berlin, 1991, p. 91.
- [99] H. Gnaser, *Low-Energy Ion Irradiation of Solid Surfaces*, Springer, Berlin, 1999.
- [100] H. Gnaser, *Phys. Rev. B* 54 (1996) 16456.
- [101] H. Gnaser, *Phys. Rev. B* 63 (2001) 045415.
- [102] H.M. Urbassek, W.O. Hofer, K. Dan, *Vidensk. Selsk. Mat. Fys. Medd.* 43 (1993) 97.
- [103] H. Gnaser, *Nucl. Instrum. Method B* 164–165 (2000) 705.
- [104] H. Gnaser, R. Golser, W. Kutschera, A. Priller, P. Steier, C. Vockenhuber, *Appl. Surf. Sci.* 231–232 (2004) 117.
- [105] R. Golser, H. Gnaser, W. Kutschera, A. Priller, P. Steier, C. Vockenhuber, *Nucl. Instrum. Method B* 223–224 (2004) 221.
- [106] R. Golser, H. Gnaser, W. Kutschera, A. Priller, P. Steier, A. Wallner, *Nucl. Instrum. Methods B*, submitted to publication.